Progress In Electromagnetics Research M, Vol. 91, 1–10, 2020

The Diffraction by Two Half-Planes and Wedge with the Fractional Boundary Condition

Vasil Tabatadze[1, *], Kamil Karaçuha[1], Eldar Veliyev[1, 2], and Ertuğrul Karaçuha[1]

Abstract—In this article, the diffraction of plane electromagnetic waves by double half-planes with fractional boundary conditions is considered. As particular cases, the diffractions by wedges and corners are considered for different values of fractional orders. The results are compared to the analytical ones. The interesting properties of wedge diffraction are outlined for intermediate fractional orders.

1. INTRODUCTION

Fractional calculus goes back to the 17th century, but its usage in applications or physical problems started in the 19th century. First, in the literature, the application of the fractional calculus in electromagnetic and diffraction problems was developed by Engheta [1–3], and then, together with Veliyev, mathematical development for the solution of scattering and diffraction problems was prepared [4–6]. Veliyev et al. proposed fractional boundary condition which is the expansion of the well-known boundary conditions, namely, Dirichlet and Neumann. The fractional boundary condition represents the intermediate states between the perfect electric conductor (corresponds to Dirichlet Boundary Condition) and the perfect magnetic conductor (corresponds to Neumann Boundary Condition) [7–9]. In general, fractional boundary condition describes the boundary with the imaginary impedance [5–7]. After that, several works concerning the diffraction of the plane wave by the one strip, two strips, and one half-plane were published [8–11].

In this study, two half-planes are investigated for different configurations explained in the following sections. In the literature, there are many studies about the wedge with different configurations and materials. In [12], a different type of electromagnetic wave diffraction by the perfect electric conductor wedges is considered. In [13], the authors investigate the canonical problem of plane wave diffraction by a wedge in the context of the spectral domain approach which exploits the relationship between the induced current on a scatterer and its far-field. In another study, for the wedge diffraction problem, there exists a new potential function. Here, the line integration which gives edge diffracted fields is constructed for wedge diffraction by using the method of the modified theory of physical optics [14]. In [15], TE and TM polarized electromagnetic wave diffraction on a perfectly conductive wedge with arbitrary apex angle is numerically studied. Besides the numerical analysis, the author in [16] considers analytical techniques for the wedge diffraction problems. Currently, in the studies, authors are considering boundary value problems for the Helmholtz equation, with complex wavenumber, admitting combinations of Dirichlet and Neumann boundary conditions related to the diffraction by the wedge [17]. Also, there exists a review of the articles related to the diffraction by the wedge, and the review is to showcase the disparate mathematical techniques that have been proposed [18].

The proposed method uses fractional calculus and its apparatus for the boundary conditions and orthogonal polynomials and spectral representation for the current densities on half-planes and field

Received 5 February 2020, Accepted 23 March 2020, Scheduled 26 March 2020

* Corresponding author: Vasil Tabatadze (vasilitabatadze@gmail.com).

[1] The Informatics Institute of Istanbul Technical University, Istanbul, Turkey. [2] National University of 'Kharkiv Polytechnic Institute', Kharkiv 61000, Ukraine.

expression, respectively. The solution of the diffraction problem is obtained by the use of the method of orthogonal polynomials (O. P.) which is quite straightforward and simpler with respect to Wiener-Hopf Technique for similar problems. This alternative method was introduced by Veliyev [19]. In this method, the scattered fields were obtained using the Fourier transform of the corresponding induced fractional surface current densities. This analytical-numerical method, using a spectral approach, reduces the problem to a system of linear algebraic equations (SLAE) for the unknown Fourier coefficients of the current density function. The convenient and appropriate truncation of SLAE can lead to the solution with any required accuracy. The advantage of the method by using the analytical and numerical methods together is to give accurate results for wide frequency range including resonance, high-frequency and low-frequency ranges. With this method, the advantages of analytical approach for high-frequency regime and the advantages of numerical approach for the high and low regimes are gathered [20].

2. FORMULATION OF THE PROBLEM

In this section, the formulation of the problem and its theoretical explanation are investigated in detail. Here, the study consists of two half-planes. The first half-plane (lower) is located at $y = 0$ starting from $x = 0$ to $x = \infty$. The second half-plane (upper) is rotated with the angle α and translates the amount of a and l in the directions of x and y, respectively. The half-planes have an infinite length in the z-direction and infinitesimal height. The incidence electric field is a uniform plane and denoted as $\vec{E}_z^i$. The incidence electric field can be expressed as $\vec{E}_z^i(x,y) = e^{-ik(x\cos\theta + y\sin\theta)}\hat{e}_z$. Note that $\hat{e}_z$ is the unit vector pointing the z-direction; θ is the angle of incidence; and $k = 2\pi/\lambda$ is the wavenumber (λ is the wavelength in free-space). Keep in mind that the time-dependency throughout the study is taken as $e^{-i\omega t}$. In Fig. 1(a), the geometry of the problem is given. In the figure, there are a global (x, y, z) and a local (x_1, y_1, z) coordinate systems. If the values of l and a are small compared to the wavelength, we get the wedge (Fig. 1(b)).

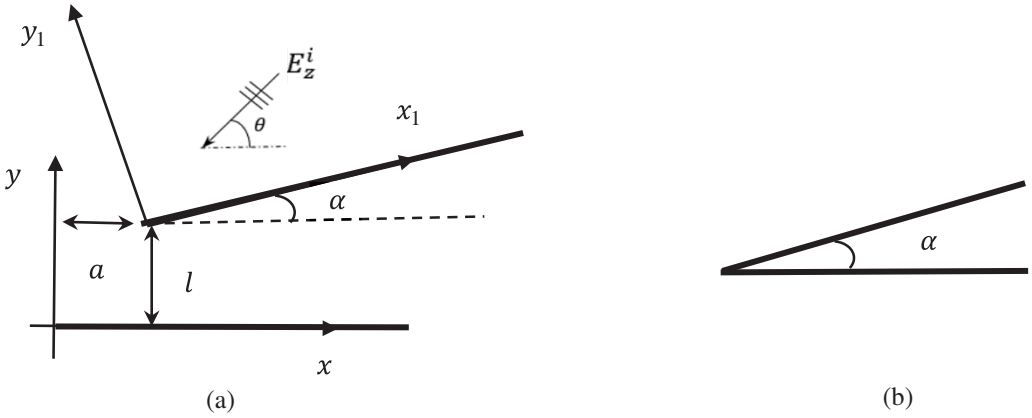

Figure 1. The geometries of the problem.

As it is known, due to having half-planes in the space and incidence electromagnetic field, the scattered fields are formed. In the space, the total electric field $E_z(x,y)$ can be expressed as Eq. (1).

$$E_z(x,y) = E_z^{s1}(x,y) + E_z^{s2}(x,y) + E_z^i(x,y) \tag{1}$$

Here, $E_z^{s1}(x,y)$ corresponds to the scattered electric field due to the horizontal half-plane located at $y = 0$, and $E_z^{s2}(x,y)$ stands for the scattered electric field due to the translated and rotated half-plane as given in Fig. 1.

In order to find the total electric field distribution, the total field is subjected to the fractional boundary condition [4–6] as given in Eq. (2) on each surface of the half-plane.

$$\begin{aligned} D_{ky}^{\nu} E_z|_{y=\pm 0} &= 0, \quad x \in [0,\infty) \\ D_{ky_1}^{\nu} E_z|_{y_1=\pm 0} &= 0, \quad x_1 \in [0,\infty) \end{aligned} \tag{2}$$

Here, D_{ky}^{ν} and $D_{ky_1}^{\nu}$ stand for the fractional derivative with respect to dimensionless parameters ky and ky_1, respectively. The derivative is in the order of ν which is called the fractional order (FO) and can have the value between (0, 1) [5–7]. Note that the derivative is taken with respect to the normal direction for each half-plane. Keep in mind that the derivative is taken by the integral of Riemann-Liouville which has the next form [21].

$$-_{\infty}D_x^{\nu}f(x) = \frac{1}{\Gamma(1-\nu)}\frac{d}{dx}\int_{-\infty}^{x}\frac{f(t)dt}{(x-t)^{\nu}}, \quad 0<\nu<1 \tag{3}$$

Here, $\Gamma(1-\nu)$ is the Gamma function. From Eq. (3), a very useful property is obtained as $D_{ky}^{\nu}e^{iky} = (i)^{\nu}e^{iky}$. After having this property, the main aim is to express all field components in terms of the exponentials. Then, the fractional boundary condition given in Eq. (2) can be taken easily.

In order to apply the boundary condition on each half-plane, the scattered electric fields need to be expressed as the convolution of the induced fractional current density with the fractional Green's function [4, 6] as given in Eq. (4).

$$\begin{aligned} E_z^{s1}(x,y) &= \int_0^{\infty} f_1^{\nu}\left(x'\right) G^{\nu}(x-x'y)dx' \\ E_z^{s2}(x_1,y_1) &= \int_a^{\infty} f_2^{\nu}\left(x_1'\right) G^{\nu}(x_1-x_1'y_1)dx_1' \end{aligned} \tag{4}$$

where, respectively:

$$\begin{aligned} G^{\nu}\left(x-x',y\right) &= -\frac{i}{4}D_{ky}^{\nu}H_0^{(1)}\left(k\sqrt{(x-x')^2+(y)^2}\right) \\ G^{\nu}\left(x_1-x_1',y_1\right) &= -\frac{i}{4}D_{ky_1}^{\nu}H_0^{(1)}\left(k\sqrt{(x_1-x_1')^2+(y_1)^2}\right) \end{aligned}$$

Here, note that $H_0^{(1)}$ is the Hankel function of the first kind and zero-order. Its spectral representation is given as follows [22]. Besides, having two-dimensional and flat geometry (half-plane), y' and y_1' are constant and equal to zero.

$$H_0^{(1)}\left(k\sqrt{(x-x')^2+(y-y')^2}\right) = \frac{1}{\pi}\int_{-\infty}^{\infty} e^{ik[(x-x')q+|y-y'|\sqrt{1-q^2}]}\frac{dq}{\sqrt{1-q^2}}$$

In order to apply the fractional boundary condition, the coordinate transform is needed, and it can be achieved as Eq. (5).

$$x_1 = Ax - By + a, \quad y_1 = Bx + Ay + l \tag{5}$$

where $A = \cos\alpha$, $B = \sin\alpha$.

The scattered field for the lower and upper half-planes can be obtained as Eq. (6) by using Eq. (4) and the spectral representation of the Hankel function [10, 11].

$$\begin{aligned} E_z^{s1}(xy) &= -\frac{i}{4\pi}e^{\pm\frac{i\pi\nu}{2}}\int_{-\infty}^{\infty} F_1^{\nu}(q)e^{ik(xq+|y|\sqrt{1-q^2})}(1-q^2)^{\frac{\nu-1}{2}}dq \quad (+\text{for } y>0 \ -\text{for } y<0) \\ E_z^{s2}(x_1y_1) &= -\frac{i}{4\pi}e^{\pm\frac{i\pi\nu}{2}}\int_{-\infty}^{\infty} F_2^{\nu}(q)\,e^{ik\left(x_1q+|y_1|\sqrt{1-q^2}\right)}\left(1-q^2\right)^{\frac{\nu-1}{2}}dq \quad (+\text{for } y_1>0 \ -\text{for } y_1<0) \end{aligned} \tag{6}$$

where,

$$F_1^{\nu}(q) = \int_0^{\infty} f_1^{\nu}\left(x'\right)e^{-ikqx'}dx', \quad F_2^{\nu}(q) = \int_0^{\infty} f_2^{\nu}\left(x_1'\right)e^{-ikqx_1'}dx_1'$$

Here, $F_1^\nu(q)$ and $F_2^\nu(q)$ are the Fourier transform of the induced fractional current densities on each half-plane, respectively.

In Eq. (7), the boundary condition is applied to the total electric field on the lower half-plane

$$D_{ky}^\nu\left(\int_0^\infty f_1^\nu(x')\,G^\nu(x-x',y)\,dx'+\int_0^\infty f_2^\nu(x_1')\,G^\nu(x_1-x_1',y_1)\,dx_1'+e^{-ik(x\cos\theta+y\sin\theta)}\right)_{y=\pm 0}=0 \quad (7)$$

Then, the final form of Eq. (7) is obtained as Eq. (8) by using Eqs. (4) and (6).

$$\begin{aligned}&-\frac{i}{4\pi}e^{\pm i\pi\nu}\left(\int_{-\infty}^\infty F_1(q)\,e^{ikxq}\left(1-q^2\right)^{\nu-\frac{1}{2}}dq\right.\\&\left.+\int_{-\infty}^\infty F_2(q)\left(-iBq\pm iA\sqrt{1-q^2}\right)^\nu e^{ik\left(Aq+B\sqrt{1-q^2}\right)x}e^{ik(aq+l\sqrt{1-q^2})}(1-q^2)^{\frac{\nu-1}{2}}dq\right)\\&=-(-i\sin\theta)^\nu e^{-ikx\cos\theta}\end{aligned} \quad (8)$$

Here, $Bx+l>0$.

In Eq. (9), the boundary condition is applied to the total electric field on the upper half-plane

$$D_{ky_1}^\nu\left(\int_0^\infty f_1^\nu(x')\,G^\nu(x-x',y)\,dx'+\int_0^\infty f_2^\nu(x_1')\,G^\nu(x_1-x_1',y_1)\,dx_1'+e^{-ik(x\cos\theta+y\sin\theta)}\right)_{y_1=\pm 0}=0 \quad (9)$$

Then, the final form of Eq. (9) is obtained as Eq. (10) by using Eqs. (4) and (6).

$$\begin{aligned}&-\frac{i}{4\pi}e^{\pm i\pi\nu}\left(\int_{-\infty}^\infty F_1(q)\,e^{ikxq}\left(1-q^2\right)^{\nu-\frac{1}{2}}dq\right.\\&\left.+\int_{-\infty}^\infty F_2(q)\left(-iBq\pm iA\sqrt{1-q^2}\right)^\nu e^{ik\left(Aq+B\sqrt{1-q^2}\right)x}e^{ik(aq+l\sqrt{1-q^2})}(1-q^2)^{\frac{\nu-1}{2}}dq\right)\\&=-(-i\sin\theta)^\nu e^{-ikx\cos\theta}\end{aligned} \quad (10)$$

Here, $-Bx_1-Al+Ba<0$ and in order to apply the boundary condition on the half-planes, the coordinate transform is required. The following transformations are employed for the scattered field and the incidence field, respectively as Eq. (11).

For the scattered electric field,

$$\begin{aligned}x&=Ax_1+By_1-Aa-Bl\\y&=-Bx_1+Ay_1+Ba-Al\end{aligned} \quad (11)$$

For the incidence wave,

$$\begin{aligned}x&=Ax_1-By_1+a\\y&=Bx_1+Ay_1+l\end{aligned}$$

where $A=\cos\alpha$, $B=\sin\alpha$.

After having coupled integral equations (IE) given in Eqs. (8) and (10), the solution methodology is introduced. Here, by taking into account the geometry of the problem and the edge condition [6, 23], the fractional current density is expressed as the summation of Laguerre polynomials with the unknown coefficients f_n^1 as given in Eq. (12). Note that the factor $e^{-\varsigma}\varsigma^{\nu-\frac{1}{2}}$ forces to satisfy the edge and radiation conditions.

$$\begin{aligned}f_1^\nu\left(\frac{\varsigma}{k}\right)&=e^{-\varsigma}\varsigma^{\nu-\frac{1}{2}}\sum_{n=0}^\infty f_n^1 L_n^{\nu-\frac{1}{2}}(2\varsigma),\varsigma=kx\\f_2^\nu\left(\frac{\varsigma}{k}\right)&=e^{-\varsigma}\varsigma^{\nu-\frac{1}{2}}\sum_{n=0}^\infty f_n^2 L_n^{\nu-\frac{1}{2}}(2\varsigma),\varsigma=kx_1\end{aligned} \quad (12)$$

Then, the Fourier transform of Eq. (12) is found as Eq. (13), respectively [6, 19].

$$\begin{aligned} F_1^{\nu}(q) &= \int_0^{\infty} f_1^{\nu}\left(x'\right) e^{-ikqx'} dx' = \frac{1}{k}\sum_{n=0}^{\infty} f_n^1 \gamma_n^{\nu} \frac{(iq-1)^n}{(iq+1)^{\nu+n+\frac{1}{2}}} \\ F_2^{\nu}(q) &= \int_0^{\infty} f_2^{\nu}\left(x_1'\right) e^{-ikqx_1'} dx_1' = \frac{1}{k}\sum_{n=0}^{\infty} f_n^2 \gamma_n^{\nu} \frac{(iq-1)^n}{(iq+1)^{\nu+n+\frac{1}{2}}} \end{aligned} \tag{13}$$

where $\gamma_n^{\nu} = \frac{\Gamma(n+\nu+\frac{1}{2})}{\Gamma(n+1)}$. Here, the following property is utilized [19, 22].

$$\int_0^{\infty} e^{-\varsigma(1+iq)} \varsigma^{\nu-\frac{1}{2}} L_n^{\nu-\frac{1}{2}}(2\varsigma)\, d\varsigma = \gamma_n^{\nu} \frac{(iq-1)^n}{(iq+1)^{\nu+n+\frac{1}{2}}}$$

After obtaining Eq. (13), $F_1^{\nu}(q)$ and $F_2^{\nu}(q)$ are inserted into Eqs. (8) and (10). Then, both sides of IE in Eqs. (8) and (10) are multiplied by $e^{-\varsigma}\varsigma^{\nu-\frac{1}{2}} L_n^{\nu-\frac{1}{2}}(2\varsigma)$ and take an integral from 0 to ∞ with respect to the variable, ς. Again, the same property given above is used. Then, IE in Eqs. (14) and (15) are obtained for the lower and upper half-planes, respectively.

IE for the lower half-plane:

$$\frac{i}{4\pi k} e^{\pm i\pi\nu} \sum_{n=0}^{\infty} f_n^1 \gamma_n^{\nu} C_{nm}^{11} (-1)^{n+m} + \frac{i}{4\pi k} e^{\frac{\pm i\pi\nu}{2}} \sum_{n=0}^{\infty} f_n^2 \gamma_n^{\nu} C_{nm}^{12} (-1)^m = (-i\sin\theta)^{\nu} \frac{(i\cos\theta - 1)^m}{(1+i\cos\theta)^{\nu+m+\frac{1}{2}}} \tag{14}$$

where,

$$C_{nm}^{11} = \int_{-\infty}^{\infty} \left(1-q^2\right)^{\nu-\frac{1}{2}} \frac{(1-iq)^{n-m-\nu-\frac{1}{2}}}{(1+iq)^{n-m+\nu+\frac{1}{2}}} dq$$

$$C_{nm}^{12} = \int_{-\infty}^{\infty} \Pi(q) \frac{(iq-1)^n}{(iq+1)^{n+m+\frac{1}{2}}} \left(-iBq \pm iA\sqrt{1-q^2}\right)^{\nu} e^{ik\left(aq+l\sqrt{1-q^2}\right)} \left(1-q^2\right)^{\frac{\nu-1}{2}} dq$$

$$\Pi(q) = \frac{\left(1+i(Aq+B\sqrt{1-q^2})\right)^m}{\left(1-i\left(Aq+B\sqrt{1-q^2}\right)\right)^{m+\nu+\frac{1}{2}}}$$

IE for the upper half-plane:

$$\begin{aligned} &\frac{i}{4\pi k} e^{\frac{\pm i\pi\nu}{2}} \left(\sum_{n=0}^{\infty} f_n^1 \gamma_n^{\nu} C_{nm}^{21} (-1)^m + \sum_{n=0}^{\infty} f_n^2 \gamma_n^{\nu} C_{nm}^{22} (-1)^{n+m}\right) \\ &= (-iB\cos\theta + iA\sin\theta)^{\nu} e^{-ik(a\cos\theta + l\sin\theta)} \frac{(i(A\cos\theta + B\sin\theta) - 1)^m}{(i(A\cos\theta + B\sin\theta) + 1)^{\nu+m+\frac{1}{2}}} \end{aligned} \tag{15}$$

where,

$$C_{nm}^{21} = \int_{-\infty}^{\infty} \Pi(q) \frac{(iq-1)^n}{(iq+1)^{n+m+\frac{1}{2}}} \left(iBq \pm iA\sqrt{1-q^2}\right)^{\nu} e^{ik(-aAq - lBq - Ba\sqrt{1-q^2} + Al\sqrt{1-q^2})} \left(1-q^2\right)^{\frac{\nu-1}{2}} dq$$

$$C_{nm}^{22} = \int_{-\infty}^{\infty} \left(1-q^2\right)^{\nu-\frac{1}{2}} \frac{(1-iq)^{n-m-\nu-\frac{1}{2}}}{(1+iq)^{n-m+\nu+\frac{1}{2}}} dq$$

3. NUMERICAL RESULTS

Based on the described mathematical algorithm, the program package was created in MatLab, and the near electric field distribution was evaluated for different parameters of the half-planes.

Figure 2 shows the total near electric field distribution for the wedge diffraction from inside. Inside the wedge structure, the standing wave is observed. Fig. 3 shows a similar case. The only difference is that the upper half-plane is shifted. Again we have standing wave inside the wedge. However, in this case, some part of the energy can go through the gap and is radiated to outer space. The fractional order in two cases corresponds to the perfect electric conductor ($\nu = 0.01$).

Figure 4 corresponds to the diffraction by the right angle corner from inside. The standing wave is observed inside. If we shift the upper half-plane and make a gap between half-planes as shown in Fig. 5, the standing wave is still preserved. Again, some part of the energy is radiated outside through the gap like in case of the wedge.

If we shift the lower half-plane, we will get the horizontal gap, and the energy will be radiated below through the gap (Fig. 6). Again, the fractional order corresponds to the perfect electric conductor. After we consider diffraction by the wedge from outside. We consider a different angle of the wedge. Fig. 7 shows the near electric field distribution for the wedge diffraction with angle $\alpha = \frac{\pi}{6}$. As we see, the

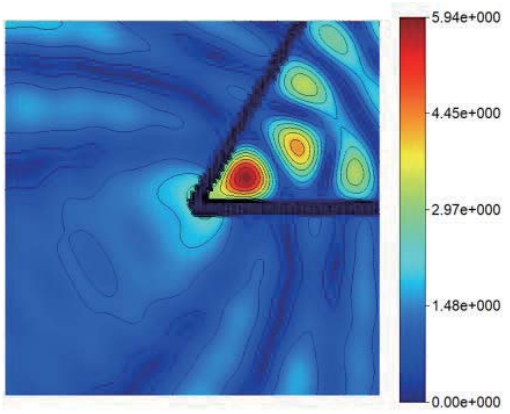

Figure 2. The total near electric field distribution (for animation see [24]) $\alpha = \frac{\pi}{3}$, $\nu = 0.01$, $\theta = \frac{\pi}{6}$, $l = 0.1$, $a = 0$.

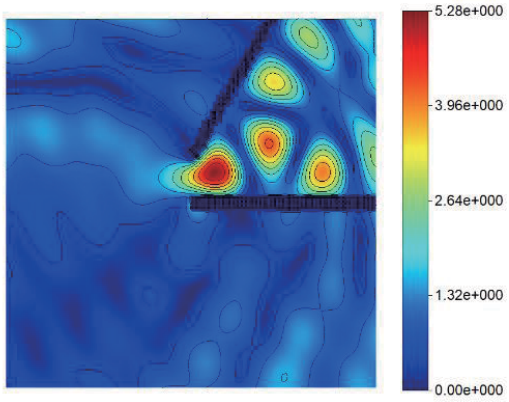

Figure 3. The total near electric field distribution (for animation see [24]) $\alpha = \frac{\pi}{3}$, $\nu = 0.01$, $\theta = \frac{\pi}{6}$, $l = \pi$, $a = 0$.

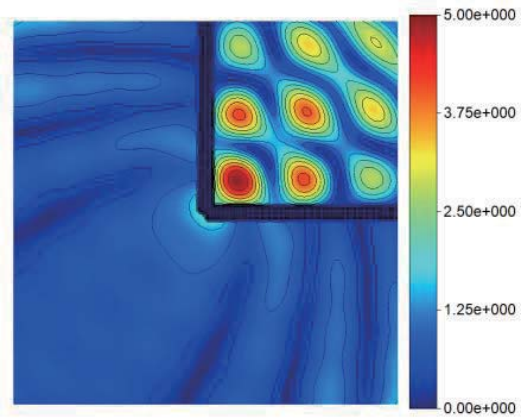

Figure 4. The total near electric field distribution (for animation see [24]) $\alpha = \frac{\pi}{2}$, $\nu = 0.01$, $\theta = \frac{\pi}{4}$, $l = 0.1$, $a = 0$.

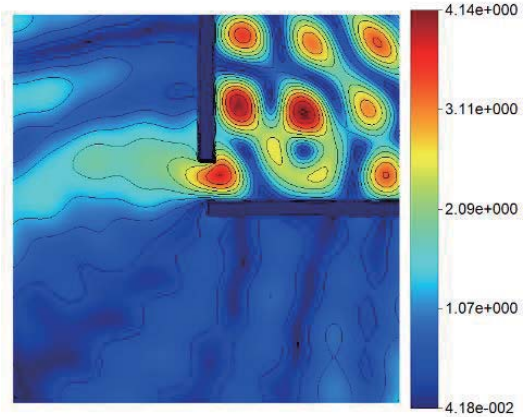

Figure 5. The total near electric field distribution (for animation see [24]) $\alpha = \frac{\pi}{2}$, $\nu = 0.01$, $\theta = \frac{\pi}{4}$, $l = \pi$, $a = 0$.

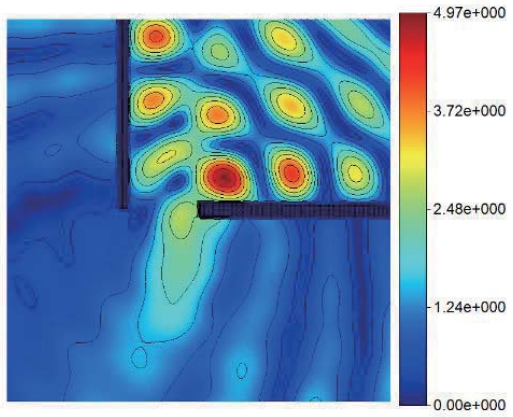

Figure 6. The total near electric field distribution (for animation see [24]) $\alpha = \frac{\pi}{2}$, $\nu = 0.01$, $\theta = \frac{\pi}{4}$, $l = 0.1$, $a = 10$.

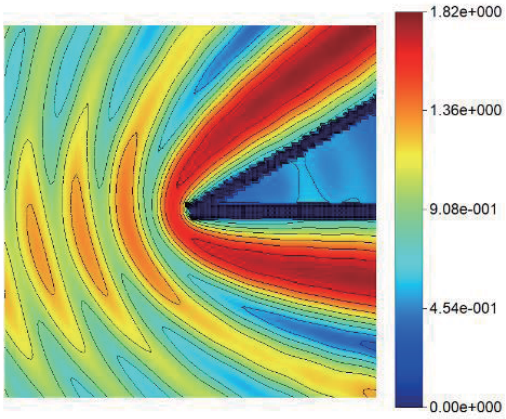

Figure 7. The total near electric field distribution (for animation see [24]) $\alpha = \frac{\pi}{6}$, $\nu = 0.01$, $\theta = \pi + \frac{\pi}{12}$, $l = 0.1$, $a = 0$.

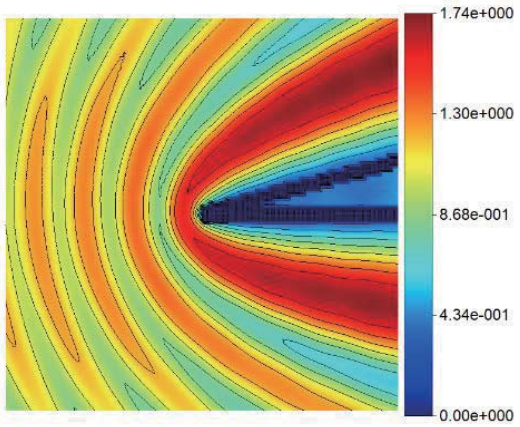

Figure 8. The total near electric field distribution (for animation see [24]) $\alpha = \frac{\pi}{12}$, $\nu = 0.01$, $\theta = \pi + \frac{\pi}{24}$, $l = 0.1$, $a = 0$.

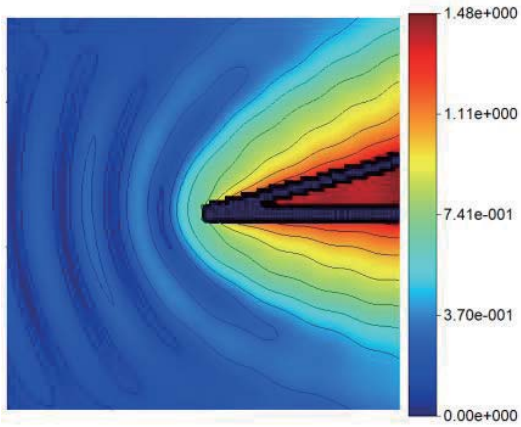

Figure 9. The scattered near electric field distribution (for animation see [24]) $\alpha = \frac{\pi}{12}$, $\nu = 0.01$, $\theta = \pi + \frac{\pi}{24}$, $l = 0.1$, $a = 0$.

field inside the wedge is practically zero. In order to verify our results, we compare it to the results obtained by the analytical formula given in the work [16]. Figs. 8 and 9 show the total and scattered near electric field distributions for the diffraction by the wedge with the angle $\alpha = \frac{\pi}{12}$ obtained by our method. Note that the backscattering is very small. Most of the scattered field goes forward.

Figures 10 and 11 show the same results obtained by the analytical formula given in the work [16]. As we see, the results obtained by the analytical formulas are pretty similar to the results obtained by our method. Analytical results do not give the correct results inside the wedge, that is why we make zero automatically. In our method there is a very small gap between the half-planes that is why we have field inside. This gap is required in order to avoid singularity in the solution. If the wavelength (λ) is much larger than the gap, our structure approximates the perfect wedge very well with no gap.

All results considered above were for perfect electric conductor. Now we will consider different values of the fractional order.

Figure 12 corresponds to the diffraction by the wedge with a gap from inside when the fractional order is $\nu = 1$, which corresponds to the perfect magnetic conductor (PMC). As we see, the field structure is quite different from the case given in Fig. 3. Fig. 13 corresponds to the diffraction by the perfect magnetic conductor wedge from outside. Again field does not penetrate inside the field

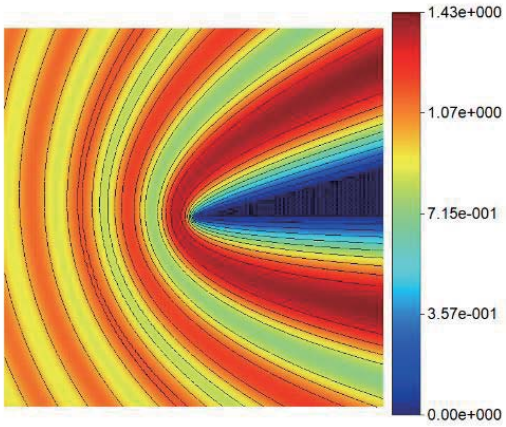

Figure 10. The total near electric field distribution, Analytic (for animation see [24]) $\alpha = \frac{\pi}{12}$, $\nu = 0.01$, $\theta = \pi + \frac{\pi}{24}$, $l = 0.1$, $a = 0$.

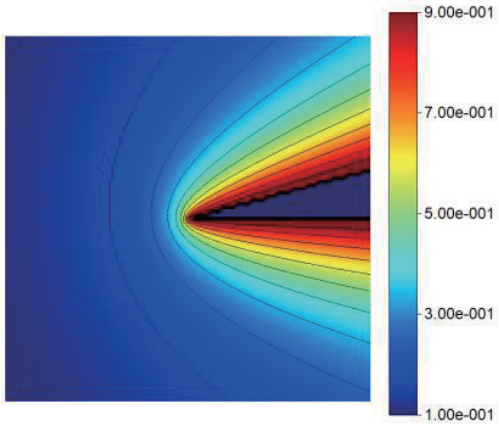

Figure 11. The scattered near electric field distribution, Analytic (for animation see [24]) $\alpha = \frac{\pi}{12}$, $\nu = 0.01$, $\theta = \pi + \frac{\pi}{24}$, $l = 0.1$, $a = 0$.

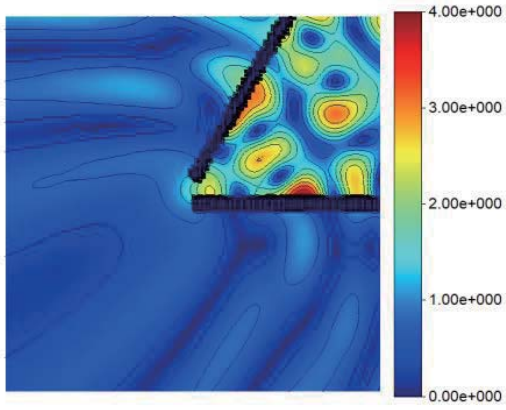

Figure 12. The total near electric field distribution (for animation see [24]) $\alpha = \frac{\pi}{3}$, $\nu = 1$, $\theta = \frac{\pi}{6}$, $l = \pi$, $a = 0$.

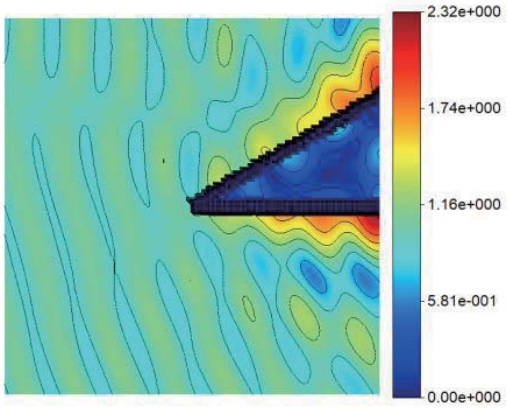

Figure 13. The total near electric field distribution (for animation see [24]) $\alpha = \frac{\pi}{6}$, $\nu = 1$, $\theta = \pi + \frac{\pi}{12}$, $l = 0.1$, $a = 0$.

amplitude and is practically zero inside the wedge.

We also considered the case for fractional order $\nu = 0.5$. Fig. 14 shows the diffraction by the corner with the right angle from inside. As the figure shows, the high field values are again inside the corner, but some part of the energy goes outside through the walls. This is the main difference if we compare it to the PEC and PMC cases. Fig. 15 shows diffraction by the wedge from outside for fractional order $\nu = 0.5$. As we can see, the field values inside the wedge are no longer minimum in contrast to the PEC and PMC cases (Fig. 7 and 13). Instead, the field distribution has maximum values inside the wedge. This property of the material with fractional order was also shown in the work [11]. It corresponds to the material with impedance $\eta = -i$. When the wave falls to this structure, this material amplifies the field and transmits to another side with a higher amplitude.

We also considered the cases of fractional order $\nu = 0.25$ and $\nu = 0.75$. The results are given in Fig. 16 and Fig. 17, respectively. Here, the diffraction by the wedge is considered, and the field inside the wedge again has a non-zero value.

All the field animations related to the results given in this article are uploaded to YouTube and can be found at the link in [24].

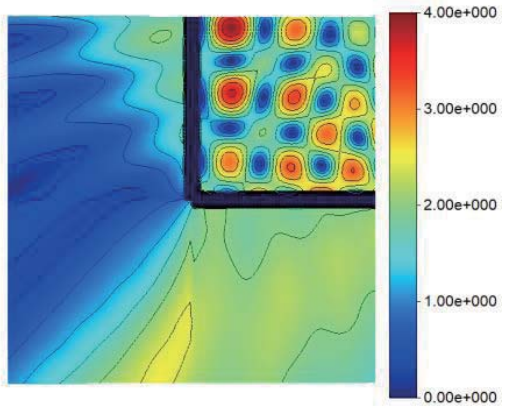

Figure 14. The total near electric field distribution (for animation see [24]) $\alpha = \frac{\pi}{2}$, $\nu = 0.5$, $\theta = \frac{\pi}{4}$, $l = 0.1$, $a = 0$.

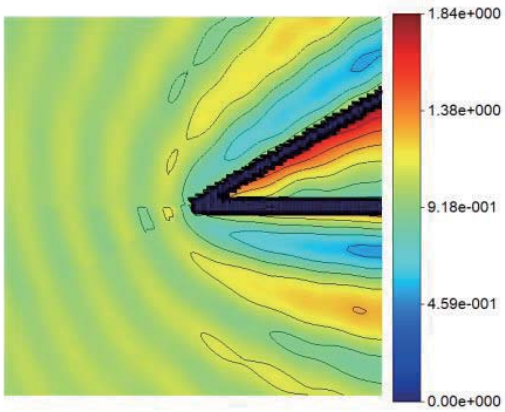

Figure 15. The total near electric field distribution (for animation see [24]) $\alpha = \frac{\pi}{6}$, $\nu = 0.5$, $\theta = \pi + \frac{\pi}{12}$, $l = 0.1$, $a = 0$.

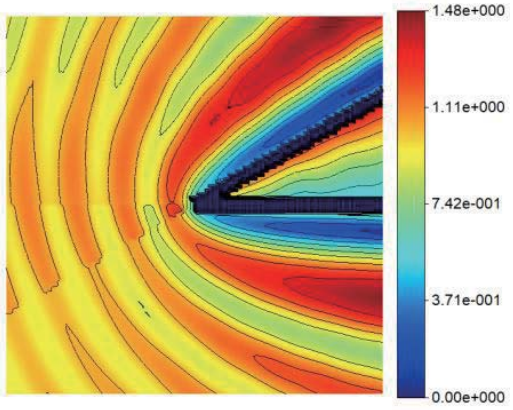

Figure 16. The total near electric field distribution (for animation see [24]) $\alpha = \frac{\pi}{6}$, $\nu = 0.25$, $\theta = \frac{\pi}{12}$, $l = 0.1$, $a = 0$.

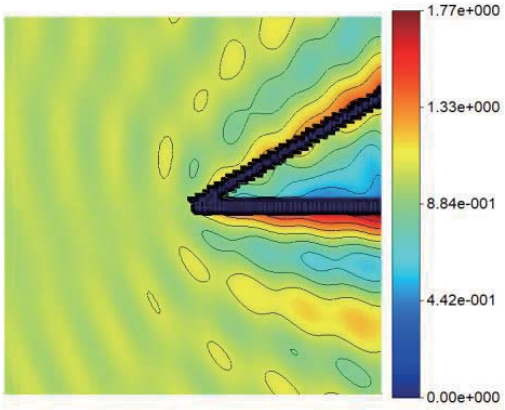

Figure 17. The total near electric field distribution (for animation see [24]) $\alpha = \frac{\pi}{6}$, $\nu = 0.75$, $\theta = \pi + \frac{\pi}{12}$, $l = 0.1$, $a = 0$.

4. CONCLUSION

In this article, the diffraction of the plane electromagnetic waves by the double half-plane is considered. The lower half-plane is fixed, and the upper one can be shifted and rotated. As particular cases, the diffraction by the wedge and corners from both sides is considered. The cases of the wedge and corners with a gap and their electromagnetic properties are also studied. Results are compared to the analytical ones. For intermediate fractional order values, interesting results are obtained. In particular, for the wedge diffraction, inside the wedge the field is not zero but has maximum which is different from PEC and PMC cases.

REFERENCES

1. Engheta, N., "Use of fractional integration to propose some "fractional" solutions for the scalar Helmholtz Equation," *Progress In Electromagnetics Research*, Vol. 12, 107–132, 1996.
2. Engheta, N., "Fractional curl operator in electromagnetics," *Microwave and Optical Technology Letters*, Vol. 17, No. 2, 86–91, 1998.

3. Engheta, N., "Phase and amplitude of fractional-order intermediate wave," *Microwave and Optical Technology Letters*, Vol. 21, No. 5, 338–343, 1999.
4. Veliev, E. I. and N. Engheta, "Generalization of Green's theorem with fractional differ-integration," *IEEE AP-S International Symposium & USNC/URSI National Radio Science Meeting*, 2003.
5. Veliev, E. I., M. V. Ivakhnychenko, and T. M. Ahmedov, "Fractional boundary conditions in plane waves diffraction on a strip," *Progress In Electromagnetics Research*, Vol. 79, 443–462, 2008.
6. Veliev, E. I., T. M. Ahmedov, and M. V. Ivakhnychenko, "Fractional operators approach and fractional boundary conditions," *Electromagnetic Waves*, V. Zhurbenko (ed.), IntechOpen, Rijeka, Croatia, 2011, doi: 10.5772/16300.
7. Veliev, E.I., K. Karacuha, and E. Karacuha, "Scattering of a cylindrical wave from an impedance strip by using the method of fractional derivatives," *XXIIIrd International Seminar/Workshop on Direct and Inverse Problems of Electromagnetic and Acoustic Wave Theory (DIPED)*,2018.
8. Karacuha, K., E. I. Veliyev, V. Tabatadze, and E. Karacuha, "Analysis of current distributions and radar cross sections of line source scattering from impedance strip by fractional derivative method," *Advanced Electromagnetics,* Vol. 8, No. 2, 108–113, 2019.
9. Tabatadze, V., K. Karacuha, and E. I. Veliev, "The fractional derivative approach for the diffraction problems: plane wave diffraction by two strips with the fractional boundary conditions," *Progress In Electromagnetics Research*, Vol. 95, 251–264, 2019.
10. Karaçuha, K., E. I. Veliyev, V. Tabatadze, and E. Karaçuha, "Application of the method of fractional derivatives to the solution of the problem of plane wave diffraction by two axisymmetric strips of different sizes," *URSI International Symposium on Electromagnetic Theory (EMTS)*, May 2019.
11. Veliyev, E. I., V. Tabatadze, K. Karaçuha, and E. Karaçuha, "The diffraction by the half-plane with the fractional boundary condition," *Progress In Electromagnetics Research M*, Vol. 88, 101–110, 2020.
12. Oberhettinger F., "On the diffraction and reflection of waves and pulses by wedges and corners," *Journal of Research of the National Bureau of Standards*, Vol. 61, No. 5, November 1958.
13. Ciarkowski, A. D., J. O. Boersma, and R. Mittra, "Plane-wave diffraction by a wedge — A spectral domain approach," *IEEETransactions On Antennas and Propagation*, Vol. 32, No. 1, 20–29, 1984.
14. Umul, Y. Z., "The theory of the boundary diffraction wave for wedge diffraction," *Journal of Modern Optics*, Vol. 55, No. 9, 1417–1426, 2008
15. Borovskii, A. V. and A. L. Galkin, "Diffraction on the wedge with an arbitrary angle," *Bulletin of the Lebedev Physics Institute*, Vol. 41, No. 1, 6–11, 2014.
16. Ufimtsev, P. Y., *Fundamentals of the Physical Theory of Diffraction*, John Wiley & Sons, 2014.
17. Castro, L. P., and D. Kapanadze, "Wave diffraction by wedges having arbitrary aperture angle," *Journal of Mathematical Analysis and Applications*, Vol. 421, No. 2, 1295–1314, 2015.
18. Nethercote, M. A., R. C. Assier, and I. D. Abrahams, "Analytical methods for perfect wedge diffraction: a review," *Wave Motion*, Vol. 93, 1024–1079, 2020
19. Veliev, E. I., "Plane wave diffraction by a half-plane: A new analytical approach," *Journal of Electromagnetic Waves and Applications*, Vol. 13, No. 10, 1439–1453, 1999.
20. Ikiz, T., S. Koshikawa, K. Kobayashi, E. I. Veliev, and A. H. Serbest, "Solution of the plane wave diffraction problem by an impedance strip using a numerical-analytical method: E-polarized case," *Journal of Electromagnetic Waves and Applications*, Vol. 15, No. 3, 315–340, Jan. 2001.
21. Samko, S. G., A. A. Kilbas, and O. I. Marichev, *Fractional Integrals and Derivatives, Theory and Applications*, Gordon and Breach Science Publishers, Langhorne, PA, USA, 1993.
22. Prudnikov, H. P., Y. H. Brychkov, and O. I. Marichev, *Special Functions, Integrals and Series*, Vol. 2, Gordon and Breach Science Publishers, 1986.
23. Honl, H., A. W. Maue, and K. Westpfahl, *Theorie der Beugung,* Springer-Verlag, Berlin, 1961.
24. *YouTube.*[Online].Available: https://www.youtube.com/watch?v=uyVNQbpx6_M&list=PLsBKZFxkreW8aznSKGKGFVvwy9RRqefwy&index=1 [Accessed: 5-Feb-2020].